Clim. Past Discuss., 8, 3015–3041, 2012
www.clim-past-discuss.net/8/3015/2012/
doi:10.5194/cpd-8-3015-2012

Climate of the Past Discussions

Two ocean states during the Last Glacial Maximum

X. Zhang, G. Lohmann, G. Knorr, and X. Xu

Alfred Wegener Institute for Polar and Marine Research, Bussestrasse 24, 27570, Bremerhaven, Germany

Received: 6 July 2012 – Accepted: 20 July 2012 – Published: 1 August 2012

Correspondence to: X. Zhang (xu.zhang@awi.de)

Published by Copernicus Publications on behalf of the European Geosciences Union.

Abstract

The last deglaciation is the best constrained global scale climate change documented by climate archives. Nevertheless, the understanding of the underlying dynamics is still limited, especially with respect to abrupt climate shifts and associated changes in the Atlantic meridional overturning circulation (AMOC). A fundamental issue is an appropriate climate state at the last glacial maximum (LGM, ~ 21 000 yr ago), which is used as initial condition for deglaciation. Using a comprehensive climate model, we show that for an identical set of LGM boundary conditions two different water mass configurations and associated AMOC states can coexist with respect to the salinity stratification in the deep Atlantic Ocean. Only one of the two ocean states is consistent with the available reconstructions, e.g. shallower AMOC and more expanded Antarctic Bottom Water. Furthermore, we also show that the salinity stratification represents a key control on the spatial configuration, the strength of the AMOC as well as the transient response of the AMOC to freshwater perturbation and therefore bears the potential to reconcile the apparent differences among models and data. In combination these findings represent a new paradigm for transient deglacial climate changes at the end of the last ice age that challenges the conventional evaluation of glacial and deglacial AMOC changes based on an ocean state derived from LGM boundary conditions.

1 Introduction

The Atlantic meridional overturning circulation (AMOC) is a key player in the climate system, due to its capability to redistribute large amounts of heat around the globe. Potential changes in the operational mode of the AMOC as a consequence of alterations in the hydrological cycle and greenhouse gas concentration draws our concerns about the future fate of our climate (Meehl et al., 2007). Research over the past decades, starting with Stommel's seminal 1961 paper (Stommel, 1961), has found a variety of stability properties of the AMOC, which were first confirmed via numerical climate

CPD
8, 3015–3041, 2012

models by Bryan (1986), Manabe and Stouffer (1988), and reviewed by Rahmstorf et al. (2005). Briefly summarized, many models suggest that the AMOC possesses a bistable regime in its parameter space, where deep-water formation can be "on" (as in present climate) or "off". As a consequence two different AMOC states can coexist at the same boundary conditions, depending on the initial conditions in the ocean. Different responses of AMOC states to changes in the hydrological cycle require the knowledge of the exact position of present climate in the bistable regime, which can be revealed by the hysteresis properties of the AMOC associated with freshwater perturbation (FWP) experiments. However, the principal difficulty for climate models is to determine the proximity of our present climate to potential thresholds (Rahmstorf et al., 2005).

Since the last glacial period, large and abrupt shifts in the AMOC have repeatedly occurred and were associated with large and abrupt changes in the climate system (e.g. Bard et al., 2000; Knorr and Lohmann, 2003). A better understanding of the AMOC stability properties in the past will shed light on our comprehension about the status of present climate and projections in the future. To investigate the underlying mechanisms, climate models are employed to simulate the last deglaciation with imposed transient boundary conditions (Liu et al., 2009). One of the most fundamental issues, in this respect, is the definition of a proper climate state used as a basis for the last deglaciation. The LGM is an excellent benchmark test-bed for climate models (Paleoclimate Modeling Intercomparison Projection, hereafter PMIP) to simulate a climate that strongly deviates from our modern condition, due to its abundance of proxy data (Adkins et al., 2002; Duplessy et al., 1988; Hesse et al., 2011; Lynch-Stieglitz et al., 2007). In the latest PMIP Phase 2 (PMIP2), however, there was a substantial difference of AMOC states among different models (Otto-Bliesner et al., 2007). Interestingly, there is no specific recipe about the initial ocean condition for LGM simulation in PMIP2. According to the bifurcation theory, it is thus open to question whether the different LGM AMOC states are potentially associated with different positions of the AMOC in a bistable regime.

CPD
8, 3015–3041, 2012

2 Model and experimental design

2.1 Model description

The comprehensive climate model COSMOS (ECHAM5-JSBACH-MPIOM), is utilized to analyse the different responses of the LGM to initial ocean states. The atmosphere model ECHAM5 (Roeckner et al., 2003), complemented by land surface model JSBACH (Brovkin et al., 2009), was utilized at T31 resolution ($\sim 3.75^{\circ}$) with 19 vertical layers. The ocean model MPI-OM (Marsland et al., 2003), including the dynamics of sea ice formulated using viscous-plastic rheology (Hibler III, 1979), has the resolution of GR30 ($\sim 3^{\circ}$) in horizontal and 40 uneven vertical layers. The climate model was already utilized to analyze the warm climate in the Miocene (Knorr et al., 2011) and the Pliocene (Stepanek and Lohmann, 2012), internal variability of climate system (Wei et al., 2012) and Holocene variability (Wei and Lohmann, 2012).

2.2 LGM experimental design

External forcing and boundary conditions are imposed according to the protocol of PMIP3 (available at http://pmip3.lsce.ipsl.fr/) for the LGM, namely: changes in orbital forcing, reduced greenhouse gas concentration (CO_2 185 ppm; N_2O 200 ppb; CH_4 350 ppb), topography and run-off route changes with respect to the blending product of ice sheet reconstruction, and changes in oceanic bathymetry and global increase of salinity by 1 psu to account for the $\sim$ 116 m sea-level lowering.

We perform two experiments LGMW and LGMS with different initial ocean states. One initialized from a present day ocean named as LGMS and the other started from a glacial ocean as LGMW. The initial glacial ocean for LGMW was generated through an ocean-only phase MPIOM (ocean component of COSMOS) which was run for 3000 years under the LGM condition. Its atmospheric forcing was derived from ECHAM4 forced by CLIMAP (CLIMAP, 1981) sea surface temperature, and initial ocean state and restoring of sea surface salinity were prescribed to CCSM 3.0 (the National Center

CPD
8, 3015–3041, 2012

for Atmospheric Research CCSM3 model) due to its good performance on LGM among the PMIP2 models (Otto-Bliesner et al., 2007). In contrast, for LGMS, the ocean state is derived from Levitus et al. (1998) to initialize COSMOS. Then under the same LGM boundary condition the fully coupled model was run 3000 and 3000 yr for LGMW and LGMS, respectively. The last 100-yr average is chosen to represent the corresponding climate scenarios.

3 Results

3.1 Surface properties in two LGM ocean states

The global mean sea surface temperatures (SST) are 14.9 °C and 15.3 °C in LGMW and LGMS, i.e. 2.8 °C and 2.4 °C lower than the pre-industrial (PI), respectively. These changes are comparable to the proxy data estimates (Waelbroeck et al., 2009) (Figs. 1 and 2). In the high latitudes of the Southern Hemisphere, our model simulates a pronounced annual mean cooling of SST around the continent (Fig. 1), in line with proxy data (Gersonde et al., 2005). In the Northern counter-part, a robust thermal gradient is well simulated around 40 ∼ 45° N, and the most pronounced cooling is found off the eastern coast of Iceland to eastern part of Nordic Sea (Fig. 1). Both features are comparable to reconstructions (Kucera et al., 2005; de Vernal et al., 2006). In contrast to MARGO data, our model and PMIP2 models underestimate the pronounced east-west SST anomaly (Waelbroeck et al., 2009). Despite the different initial conditions in LGMW and LGMS, there is also a reasonable agreement between the sea ice concentrations (SIC) in both LGM runs and proxy data (Gersonde et al., 2005) (Fig. 2a, c), such as the austral winter sea ice (WSI) extent in the Atlantic sector and the austral summer sea ice (SSI) extent in the Indian sector (Gersonde et al., 2005). But the simulations underestimate the large extent of SSI between 5° E and 5° W. The boreal WSI shows an important increase, especially along the coast of Newfoundland, extending far into the Western Atlantic (Kucera et al., 2005; de Vernal et al., 2006). The WSI extent in the

CPD
8, 3015–3041, 2012

North-Eastern Atlantic is also underestimated, resulting from an active North Atlantic drift, which maintains relatively warming condition at the sea surface (Fig. 3) (Paul and Schäfer-Neth, 2003). During boreal summer the eastern part of the Nordic Seas is partly sea ice free (Fig. 2a, c), which is spatially coherent with sea ice free conditions as indicated in the GLAMAP reconstruction of the LGM (Paul and Schäfer-Neth, 2003). In addition, there is perennial SSI extent in the west of Nordic Sea along the eastern coast of Greenland and Labrador Sea (Fig. 2), in agreement with the reconstruction (Kucera et al., 2005; de Vernal et al., 2006).

3.2 Internal properties in two LGM ocean states

The ocean interior in LGMW and LGMS shows pronounced differences in the water mass properties. Simulation LGMW displays an important key signature of the glacial ocean with the coldest and saltiest deep water at the bottom of Southern Ocean. This is consistent with a reconstruction of Adkins et al (2002), while LGMS is more similar to the present-day ocean configuration (Fig. 3). Importantly, these two classes of water mass configurations (i.e. well-stratified glacial ocean, LGMW, and present-day like ocean, LGMS) in our model simulations were also found in PMIP2 models (Fig. 4). According to water mass configuration reconstructed from nutrient tracers (Duplessy et al., 1988; Hesse et al., 2011; Lynch-Stieglitz et al., 2007), North Atlantic Deep Water (NADW) shoals to 2000–2500 m as Glacial North Atlantic Intermediate Water (GNAIW) due to the northward invasion of Antarctic Bottom Water (AABW) at the LGM. In LGMW, the upper cell of the AMOC associated with the sinking of NADW (hereafter NADW-cell) shoals by $\sim$ 500 m relative to present day, indicative of a shallow GNAIW (Duplessy et al., 1988; Hesse et al., 2011; Lynch-Stieglitz et al., 2007), meanwhile the lower cell of AMOC (hereafter AABW-cell) occupies the water column below 2500 m (Fig. 3a, d, f). However, the NADW-cell in LGMS deepens to $\sim$ 3000 m, which is even deeper than today and linked with a stronger NADW formation (Fig. 3b, e, h). In our LGM runs, enhanced southern westerlies (Fig. S1 in Supplement) results in a stronger NADW-cell due to a stronger Drake Passage Effect (Toggweiler and Samuels, 1995), which was

CPD
8, 3015–3041, 2012

also found in the present climate in using the same model (Wei et al., 2012). Furthermore, stronger net evaporation in the Atlantic catchment area (Fig. S2 in Supplement) combined with more heat loss to the atmosphere from the convection sites over the North Atlantic (Fig. S3 in Supplement) also results in an enhanced NADW-cell. In addition, the formation of Antarctic Bottom Water (AABW) as a result of sinking of surface brine during sea-ice formation is enhanced due to extensive sea ice formation and robust sea-ice export during the LGM (Shin et al., 2003) (Fig. 5). As a result, an ocean state similar to LGMS should be induced (Fig. 3b, e, h). However, the preformed strong stratification in LGMW constrains the ocean circulation and water mass configuration (Fig. 3a, d, f), leading to a much more consistent ocean state according to the proxy data, e.g. shallower deep water formation in the North Atlantic Ocean (Duplessy et al., 1988; Hesse et al., 2011; Lynch-Stieglitz et al., 2007). Thus, the resulting LGM ocean state is sensitive to the initial ocean conditions/stratification. To check whether the initial ocean-dependent feature is also available to pre-industrial simulation (control run), we have performed the additional simulation LGM2PI. In this experiment identical boundary conditions as our pre-industrial control run have been applied, but the ocean was initialised from the glacial ocean and integrated for 3000 yr. The ocean structure is very similar to our PI control run (Fig. 6), which indicates monostable behaviour with respect to the vertical ocean structure in contrast to the bistable glacial characteristics. Herein we suggest that model simulations of the LGM should be initialized from a well-stratified ocean state to enable a coherent model intercomparison and relation to data.

3.3 Transient mechanism between two LGM ocean states

Previous studies about the hysteresis properties/bifurcation of the AMOC are mainly based on FWP experiments (Bryan, 1986; Ganopolski and Rahmstorf, 2001; Manabe and Stouffer, 1988; Prange et al., 2002; Rahmstorf et al., 2005). In these experiments, the key variable governing the transition from one state to another are changes in the hydrological cycle. To investigate the potential transition in our two LGM ocean states, two FWP experiments (i.e. 0.2 Sv and 1 Sv last for 150 and 100 yr, respectively) are

CPD
8, 3015–3041, 2012

introduced into the Ice-Rafted Debris belts in the north Atlantic (Hemming, 2004). However, neither of them is able to trigger the transition between these two states (Fig. 7), implying that the two states are independent with respect to the hydrological cycle. Furthermore, the vertical structure of ocean interior in both runs is still distinctive during and after the hosing experiments. After the FWP, the AMOC in LGMW overshoots for several decades but not in LGMS case (Figs. 7 and 8), indicating an important role of the ocean stratification on the overshoot during the AMOC recovery. This is in agreement with previous model simulations indicating that the vertical ocean structure in the North Atlantic is of paramount importance to the magnitude and rapidity of abrupt climate changes during the last deglaciation (Barker et al., 2010; Knorr and Lohmann, 2007; Liu et al., 2009). After the AMOC recovery, both runs restore to their former AMOC states (Fig. 10), consistent with the hypothesis of a monostable freshwater regime during the glacials (Ganopolski and Rahmstorf, 2001; Prange et al., 2002; Romanova et al., 2004).

In our LGM runs, an intriguing pattern is that there is an upward tongue of relative saline water at the bottom of Southern Ocean (Fig. 3d, e), implying a possible passage of bottom water ventilated to the surface due to Ekman suction resulting from the strengthened overlying southern westerlies. The extent, to which the upwelling affects ocean stratification and the ocean circulation, is critical to understand the mechanism by which the transition between these two states happens. Therefore, the LGMW run was continued for another 500 yr to evaluate the resulting changes in the ocean. As expected, the entire deep-water mass becomes fresher due to vertical mixing associated with upwelling in the Southern Ocean while water mass in the upper layer becomes more saline (Fig. 9a). Moreover, temperature in the ocean interior increases (Fig. 9b), together with an enhanced AMOC resulting from the weakened stratification (Fig. 10). Therefore, changes in interior structure of LGMW ocean have a tendency towards the state in LGMS, which would be accomplished in a long diffusive time scale ($10^3 \sim 10^4$ yr).

CPD
8, 3015–3041, 2012

4 Discussion and conclusions

Using different initial ocean conditions to initialize our earth system model, we found that two LGM ocean states can coexist under identical 21 ka BP boundary. Both of them capture the main features of LGM SST and SIC patterns (Gersonde et al., 2005; Kucera et al., 2005; Paul and Schäfer-Neth, 2003; de Vernal et al., 2006; Waelbroeck et al., 2009). However, only the ocean state initialized from a preformed well-stratified ocean, reproduces a reliable interior ocean structure, e.g. shallower AMOC (Curry and Oppo, 2005; Duplessy et al., 1988; Lynch-Stieglitz et al., 2007). In previous model studies, a well-reconstructed glacial ocean can be generated if anomalies of salinity/sea ice export was imposed to the glacial Southern Ocean (Hesse et al., 2011; Paul and Schäfer-Neth, 2003), implying that the LGM boundary forcing alone may not result in an internal ocean pattern as inferred from reconstructions. The data based reconstructions shows evidence that during the LGM δ^{13}C-depleted and nutrient-rich water mass dominates the bottom of Atlantic basin, known as the northward invasion of enhanced AABW which is the cause of shoaling AMOC (Curry and Oppo, 2005; Duplessy et al., 1988; Hesse et al., 2011; Lynch-Stieglitz et al., 2007). These available data support the existence of this ocean configuration during the LGM. In agreement with a recent study by Schmitt et al. (2012) showing essentially constant atmospheric δ^{13}C during the LGM, our model results also indicate that the glacial ocean configuration recorded in the sediment might not be formed then. Therefore, coexistence of two LGM ocean states, of which the one started from preformed glacial ocean is consistent with proxy data, provides direct climate modeling evidence supporting the possibility of glacial ocean formation prior to the LGM.

LGM boundary condition can maintain two different LGM ocean states, but the realistic ocean state (i.e. LGMW) is quasi-stable due to the persistent upwelling in the Southern Ocean. Previous studies revealed that old ^{14}C signals of upwelled AABW might be detected in the sediment cores at intermediate water depth bathing in Antarctic intermediate water (AAIW) and sub-Antarctic mode water (SAMW) in the Atlantic

CPD
8, 3015–3041, 2012

sector of Southern Ocean (e.g. Skinner et al., 2010) and Arabian Sea (Bryan et al., 2010) during last deglaciation. During the LGM, the cores also recorded increasing ^{14}C ages in support of the existing upwelling in the Southern Ocean during the LGM. In addition, the increasing CO_2 concentrations during the LGM (e.g. Ahn and Brook, 2008) might also be related to the persistent upwelling in the Southern Ocean which is the key area where CO_2 was released to the atmosphere during the last deglaciation (e.g. Anderson et al., 2009). The robust upwelling in the Southern Ocean in LGMW (Fig. 12) also implicates that the ocean state during 21 ka BP was in a transient phase with slow changes in the carbon reservoir in the deep ocean. Following the LGM, the enhanced upwelling associated with cold events (e.g. Heinrich Stadial 1) in the Northern Hemisphere enhances the CO_2 release from a CO_2-supersaturated deep water reservoir in Southern Ocean (Anderson et al., 2009), which potentially provides the additional global warming necessary for termination to occur (Barker et al., 2009; Wolff et al., 2009). To date, deglacial model studies mainly focused on the LGM as the classical starting point and the LGM has also served as a benchmark time slice for model intercomparisons (Otto-Bliesner et al., 2007). However, our simulations suggest that the ocean state during the LGM was already in a transient phase. This indicates that the glacial ocean must have been generated well before the LGM, which represents a new paradigm for transient deglacial climate changes at the end of the last ice age.

An open question that has not yet been addressed is when the glacial ocean (LGM) was formed. According to previous studies, the formation of the glacial ocean is related to extensive sea-ice formation and export in the Southern Ocean, which enhances the rejection of surface brine subsiding into the deep ocean as AABW (Hesse et al., 2011; Shin et al., 2003). Using a sea-ice reconstruction based on diatoms, Allen et al. (2011) suggested that more extensive sea ice extent was found between ~ 22 ka and ~ 30 ka overlapping with the minimum temperature in Antarctica (e.g. Jouzel et al., 2007). This indicates that the brine rejection due to sea-ice formation might be stronger than during the LGM, resulting in a stronger AABW formation. At the beginning of Marine Isotope State 2 (MIS2, ~ 28 ka BP), a sharp decrease of CO_2 (Ahn and Brook, 2008) and

CPD
8, 3015–3041, 2012

benthic $\delta^{13}C$ (Hodell et al., 2003) implicates a possible formation of an abyssal carbon reservoir. Subsequently, Heinrich Event 2 was accompanied by a weaker AMOC and northward invasion of AABW (Gutjahr and Lippold, 2011), which supported the formation of the glacial ocean structure. Another potential candidate is MIS4, about 70 000 yr before present, which was also marked by the pronounced and abrupt drop of CO_2 (Ahn and Brook, 2008) and benthic $\delta^{13}C$ (Hodell et al., 2003). The temperatures in the Southern Ocean also reached a low level comparable to the LGM (e.g. Jouzel et al., 2007). Analyzing ice-core data, Bereiter et al. (2012) suggested that a mode change of millennial CO_2 variability during last glacial cycle should be linked to the formation of a glacial ocean during the MIS4. Considering the aforementioned possibilities, the process with respect to the glacial ocean formation might be much more complicated than what we expected before (Liu et al., 2005). To fully understand the formation of the glacial ocean, we still need further data and model studies related to key intervals of the last glacial/interglacial cycle.

In summary, our study combined with the available proxy evidence (e.g. Allen et al., 2011; Duplessy et al., 1988; Hodell et al., 2003; Jouzel et al., 2007; Schmitt et al., 2012), suggests that the signature of the glacial ocean interior has been formed under boundary conditions different to those of the LGM. One may speculate that the formation occurred some tens of thousands years ago when the sharpest transition from NADW to GNAIW happened (Ahn and Brook, 2008; Bereiter et al., 2012; Hodell et al., 2003). Furthermore, we suggest that during the LGM the climate system was already on its way to the equilibrium with the coeval boundary condition via persistent upwelling in the Southern Ocean, representing a new paradigm for transient deglacial climate changes at the end of the last ice age. Based on the unique behaviour of the LGM Ocean, special caution is necessary in the interpretation of glacial/deglacial climate simulations.

CPD
8, 3015–3041, 2012

Supplementary material related to this article is available online at: http://www.clim-past-discuss.net/8/3015/2012/cpd-8-3015-2012-supplement.pdf.

Acknowledgement. We thank the colleagues in Paleoclimate Dynamics group in the Alfred Wegener Institute for the Polar and Marine Research (AWI) in Bremerhaven for useful discussions. Thanks to Stephan Hageman in the Max Plank Institute in Hamburg for the HD model and the computer center of the AWI for the help in running the AWI supercomputer. X. Zhang was funded by China Scholarship Council (CSC) and the AWI. G. Lohmann was funded through the PACES program of the AWI in the Holmholtz society in Germany. G. Knorr was funded by REKLIM. Thanks go furthermore to scientists in the PMIP for providing us with their data.

References

Adkins, J. F., McIntyre, K., and Schrag, D. P.: The salinity, temperature, and delta18O of the glacial deep ocean, Science, 298, 1769–1773, doi:10.1126/science.1076252, 2002.

Ahn, J. and Brook, E. J.: Atmospheric CO_2 and climate on millennial time scales during the last glacial period, Science, 83, 83–85, doi:10.1126/science.1160832, 2008.

Allen, C. S., Pike, J., and Pudsey, C. J.: Last glacial–interglacial sea-ice cover in the SW Atlantic and its potential role in global deglaciation, Quaternary Sci. Rev., 30, 2446–2458, doi:10.1016/j.quascirev.2011.04.002, 2011.

Anderson, R. F., Ali, S., Bradtmiller, L. I., Nielsen, S. H. H., Fleisher, M. Q., Anderson, B. E., and Burckle, L. H.: Wind-driven upwelling in the Southern Ocean and the deglacial rise in atmospheric CO_2, Science, 323, 1443–1448, doi:10.1126/science.1167441, 2009.

Bard, E., Rostek, F., Turon, J.-L., and Gendreau, S.: Hydrological impact of Heinrich Events in the Subtropical Northeast Atlantic, Science, 289, 1321–1324, doi:10.1126/science.289.5483.1321, 2000.

Barker, S., Diz, P., Vautravers, M. J., Pike, J., Knorr, G., Hall, I. R., and Broecker, W. S.: Interhemispheric Atlantic seesaw response during the last deglaciation, Nature, 457, 1097–102, doi:10.1038/nature07770, 2009.

CPD
8, 3015–3041, 2012

Barker, S., Knorr, G., Vautravers, M. J., Diz, P., and Skinner, L. C.: Extreme deepening of the Atlantic overturning circulation during deglaciation, Nat. Geosci., 3, 567–571, doi:10.1038/ngeo921, 2010.

Bereiter, B., Lüthi, D., Siegrist, M., Schüpbach, S., Stocker, T. F., and Fischer, H.: Mode change of millennial CO_2 variability during the last glacial cycle associated with a bipolar marine carbon seesaw, Proc. Natl. Acad. Sci. USA, 109, 9755–9760, doi:10.1073/pnas.1204069109, 2012.

Brovkin, V., Raddatz, T., Reick, C. H., Claussen, M., and Gayler, V.: Global biogeophysical interactions between forest and climate, Geophys. Res. Lett., 36, 1–5, doi:10.1029/2009GL037543, 2009.

Bryan, F.: High-latitude salinity effects and interhemispheric thermohaline circulations, Nature, 323, 301–304, 1986.

Bryan, S. P., Marchitto, T. M., and Lehman, S. J.: The release of ^{14}C-depleted carbon from the deep ocean during the last deglaciation: evidence from the Arabian Sea, Earth Planet. Sci. Lett., 298, 244–254, doi:10.1016/j.epsl.2010.08.025, 2010.

Climap, P. M.: Seasonal reconstruction of the Earth's surface at the Last Glacial Maximum, Geol. Soc. Amer. Map Chart Ser., MC-36, 17, 1981.

Curry, W. B. and Oppo, D. W.: Glacial water mass geometry and the distribution of δ^{13}C of ΣCO_2 in the Western Atlantic Ocean, Paleoceanography, 20, 1–13, doi:10.1029/2004PA001021, 2005.

de Vernal, A., Rosell-Melé, A., Kucera, M., Hillaire-Marcel, C., Eynaud, F., Weinelt, M., Dokken, T., and Kageyama, M.: Comparing proxies for the reconstruction of LGM sea-surface conditions in the Northern North Atlantic, Quaternary Sci. Rev., 25, 2820–2834, doi:10.1016/j.quascirev.2006.06.006, 2006.

Duplessy, J. C., Shackleton, N. J., Fairbanks, R. G., Labeyriefi, L., Oppo, D., and Kallel, N.: Deepwater source variations during the last climatic cycle and their impact on the global deepwater circulation, Paleoceanography, 3, 343–360, 1988.

Ganopolski, A. and Rahmstorf, S.: Rapid changes of glacial climate simulated in a coupled climate model, Nature, 409, 153–158, doi:10.1038/35051500, 2001.

Gersonde, R., Crosta, X., Abelmann, A., and Armand, L.: Sea-surface temperature and sea ice distribution of the Southern Ocean at the EPILOG Last Glacial Maximum – a circum-Antarctic view based on siliceous microfossil records, Quaternary Sci. Rev., 24, 869–896, doi:10.1016/j.quascirev.2004.07.015, 2005.

CPD
8, 3015–3041, 2012

Gordon, C., Cooper, C., Senior, C., and Banks, H.: The simulation of SST , sea ice extents and ocean heat transports in a version of the Hadley Centre coupled model without flux adjustments, Clim. Dynam., 16, 147–168, 2000.
Gutjahr, M. and Lippold, J.: Early arrival of southern source water in the deep North Atlantic prior to Heinrich event 2, Paleoceanography, 26, 1–9, doi:10.1029/2011PA002114, 2011.
Hasumi, H. and Emori, S.: K-1 coupled model (MIROC) description, Cent. for Clim. Sys. Res., Univ. of Tokyo, K-1 Tech. Rep. 1., 34 pp., 2004.
Hemming, S.: Heinrich Events: massive late pleistocene detritus layers of the North Atlantic and their global climate imprint, Rev. Geophys., 42, RG1005, doi:10.1029/2003RG000128, 2004.
Hesse, T., Butzin, M., Bickert, T., and Lohmann, G.: A model-data comparison of δ^{13}C in the glacial Atlantic Ocean, Paleoceanography, 26, PA3220, doi:10.1029/2010PA002085, 2011.
Hibler III, W.: A dynamic thermodynamic sea ice model, J. Phys. Oceanogr., 9, 815–846, 1979.
Hodell, D. A., Venz, K. A., Charles, C. D., and Ninneman, U. S.: Pleistocene vertical carbon isotope and carbonate gradients in the South Atlantic sector of the Southern Ocean, Geochem. Geophy. Geosy., 4, 1004, doi:10.1029/2002GC000367, 2003.
Jouzel, J., Masson-Delmotte, V., Cattani, O., Dreyfus, G., Falourd, S., Hoffmann, G., Minster, B., Nouet, J., Barnola, J. M., Chappellaz, J., Fischer, H., Gallet, J. C., Johnsen, S., Leuenberger, M., Loulergue, L., Luethi, D., Oerter, H., Parrenin, F., Raisbeck, G., Raynaud, D., Schilt, A., Schwander, J., Selmo, E., Souchez, R., Spahni, R., Stauffer, B., Steffensen, J. P., Stenni, B., Stocker, T. F., Tison, J. L., Werner, M., and Wolff, E. W.: Orbital and millennial Antarctic climate variability over the past 800 000 years, Science, 317, 793–796, doi:10.1126/science.1141038, 2007.
Knorr, G. and Lohmann, G.: Southern Ocean origin for the resumption of Atlantic thermohaline circulation during deglaciation, Nature, 424, 532–536, doi:10.1038/nature01855., 2003.
Knorr, G. and Lohmann, G.: Rapid transitions in the Atlantic thermohaline circulation triggered by global warming and meltwater during the last deglaciation, Geochem. Geophy. Geosy., 8, Q12006, doi:10.1029/2007GC001604, 2007.
Knorr, G., Butzin, M., Micheels, A., and Lohmann, G.: A warm Miocene climate at low atmospheric CO_2 levels, Geophys. Res. Lett., 38, 1–5, doi:10.1029/2011GL048873, 2011.
Kucera, M., Weinelt, M., Kiefer, T., Pflaumann, U., Hayes, A., Weinelt, M., Chen, M.-T., Mix, A. C., Barrows, T. T., Cortijo, E., Duprat, J., Juggins, S., and Waelbroech, C.: Reconstruction of sea-surface temperatures from assemblages of planktonic foraminifera:

CPD
8, 3015–3041, 2012

multi-technique approach based on geographically constrained calibration data sets and its application to glacial Atlantic and Pacific Oceans, Quaternary Sci. Rev., 24, 951–998, doi:10.1016/j.quascirev.2004.07.014, 2005.

Liu, Z., Shin, S.-I., Webb, R. S., Lewis, W., and Otto-Bliesner, B. L.: Atmospheric CO_2 forcing on glacial thermohaline circulation and climate, Geophys. Res. Lett., 32, 32–35, doi:10.1029/2004GL021929, 2005.

Liu, Z., Otto-Bliesner, B. L., He, F., Brady, E. C., Tomas, R., Clark, P. U., Carlson, A. E., Lynch-Stieglitz, J., Curry, W., Brook, E., Erickson, D., Jacob, R., Kutzbach, J., and Cheng, J.: Transient simulation of last deglaciation with a new mechanism for Bolling-Allerod warming, Science, 325, 310–314, doi:10.1126/science.1171041, 2009.

Lynch-Stieglitz, J., Adkins, J. F., Curry, W. B., Dokken, T., Hall, I. R., Herguera, J. C., Hirschi, J. J.-M., Ivanova, E. V., Kissel, C., Marchal, O., Marchitto, T. M., McCave, I. N., McManus, J. F., Mulitza, S., Ninnemann, U., Peeters, F., Yu, E. F., and Zahn, R.: Atlantic meridional overturning circulation during the Last Glacial Maximum, Science, 316, 66–69, doi:10.1126/science.1137127, 2007.

Manabe, S. and Stouffer, R. J.: Two stable equilibria of a coupled ocean-atmosphere model, J. Clim., 1, 841–866, 1988.

Marsland, S. J., Haak, H., Jungclaus, J. H., Latif, M., and Röske, F.: The Max-Planck-Institute global ocean/sea ice model with orthogonal curvilinear coordinates, Ocean Model., 5, 91–127, doi:10.1016/S1463-5003(02)00015-X, 2003.

Meehl, G. A., Stocker, T. F., Collins, W. D., Friedlingstein, P., Gaye, A. T., Gregory, J. M., Kitoh, A., Knutti, R., Murphy, J. M., Noda, A., Raper, S. C. B., Watterson, I. G., Weaver, A. J., and Zhao, Z. C.: Global climate projections, in: Climate Change 2007: The Physical Science Basis. Contribution of Working Group I to the Fourth Assessment Report of the Intergovernmental Panel on Climate Change, edited by: Solomon, S., Qin, D., Manning, M., Chen, Z., Marquis, M., Averyt, K. B., Tignor, M., and Miller, H. L., Cambridge Univ. Press, New York, USA, 2007.

Otto-Bliesner, B. L., Brady, E. C., Clauzet, G., Tomas, R., Levis, S., and Kothavala, Z.: Last glacial maximum and holocene climate in CCSM3, J. Clim., 19, 2526–2544, doi:10.1175/JCLI3748.1, 2006.

Otto-Bliesner, B. L., Hewitt, C. D., Marchitto, T. M., Brady, E., Abe-Ouchi, A., Crucifix, M., Murakami, S., and Weber, S. L.: Last glacial maximum ocean thermohaline circulation:

CPD
8, 3015–3041, 2012

PMIP2 model intercomparisons and data constraints, Geophys. Res. Lett., 34, L12706, doi:10.1029/2007GL029475, 2007.
Paul, A. and Schäfer-Neth, C.: Modeling the water masses of the Atlantic Ocean at the Last Glacial Maximum, Paleoceanography, 18, 1058, doi:10.1029/2002PA000783, 2003.
Prange, M., Romanova, V., and Lohmann, G.: The glacial thermohaline circulation: stable or unstable?, Geophys. Res. Lett., 29, 2028, doi:10.1029/2002GL015337, 2002.
Rahmstorf, S., Crucifix, M., Ganopolski, A., Goosse, H., Kamenkovich, I., Knutti, R., Lohmann, G., Marsh, R., Mysak, L. A., Wang, Z., and Weaver, A. J.: Thermohaline circulation hysteresis: a model intercomparison, Geophys. Res. Lett., 32, L23605, doi:10.1029/2005GL023655, 2005.
Roeckner, E., Bäuml, G., Bonaventura, L., Brokopf, R., Esch, M., Giorgetta, M., Hagemann, S., Kirchner, I., Kornblueh, L., Manzini, E., Rhodin, A., Schlese, U., Schulzweida, U., and Tompkins, A.: The atmohspheric general circulation model, ECHAM5 Part 1: Model Description, Max Planck Institute for Meteorology, Hamburg, MPI Report No. 349, 127 pp., 2003.
Romanova, V., Prange, M., and Lohmann, G.: Stability of the glacial thermohaline circulation and its dependence on the background hydrological cycle, Clim. Dynam., 22, 527–538, doi:10.1007/s00382-004-0395-z, 2004.
Schmitt, J., Schneider, R., Elsig, J., Leuenberger, D., Lourantou, A., Chappellaz, J., Köhler, P., Joos, F., Stocker, T. F., Leuenberger, M. and Fischer, H.: Carbon isotope constraints on the deglacial CO_2 rise from ice cores, Science, 336, 711–714, doi:10.1126/science.1217161, 2012.
Shin, S.-I., Liu, Z., Otto-Bliesner, B. L., Kutzbach, J., and Vavrus, S. J.: Southern Ocean sea-ice control of the glacial North Atlantic thermohaline circulation, Geophys. Res. Lett., 30, 1096, doi:10.1029/2002GL015513, 2003.
Skinner, L. C., Fallon, S., Waelbroeck, C., Michel, E., and Barker, S.: Ventilation of the deep Southern Ocean and deglacial CO_2 rise, Science, 328, 1147–1151, doi:10.1126/science.1183627, 2010.
Stepanek, C. and Lohmann, G.: Modelling mid-Pliocene climate with COSMOS, Geosci. Model Dev. Discuss., 5, 917–966, doi:10.5194/gmdd-5-917-2012, 2012.
Stommel, H.: Thermohaline convection with two stable regimes of flow, Tellus, 13, 224–230, 1961.
Toggweiler, J. R. and Samuels, B.: Effect of Drake Passage on the global thermohaline circulation, Deep Sea Res. Pt. I, 42, 477–500, 1995.

CPD
8, 3015–3041, 2012

Waelbroeck, C., Paul, A., Kucera, M., Rosell-Melé, A., Weinelt, M., Schneider, R., Mix, A. C., Abelmann, A., Armand, L., Bard, E., Barker, S., Barrows, T. T., Benway, H., Cacho, I., Chen, M. T., Cortijo, E., Crosta, X. de Vernal, A., Dokken, T., Duprat, J., Elderfield, H., Eynaud, F., Gersonde, R., Hayes, A., Henry, M., Hillaire-Marcel, C., Huang, C. C., Jansen, E., Juggins, S., Kallel, N., Kiefer, T., Kienast, M., Labeyrie, L., Leclaire, H., Londeix, L., Mangin, S., Matthiessen, J., Marret, F., Meland, M., Morey, A. E., Mulitza, S., Pflaumann, U., Pisias, N. G., Radi, T., Rochon, A., Rohling, E. J., Sbaffi, L., Schäfer-Neth, C., Solignac, S., Spero, H., Tachikawa, K., Turon, J. L.: Constraints on the magnitude and patterns of ocean cooling at the Last Glacial Maximum, Nat. Geosci., 2, 127–132, doi:10.1038/ngeo411, 2009.

Weber, S. L., Drijfhout, S. S., Abe-Ouchi, A., Crucifix, M., Eby, M., Ganopolski, A., Murakami, S., Otto-Bliesner, B., and Peltier, W. R.: The modern and glacial overturning circulation in the Atlantic ocean in PMIP coupled model simulations, Clim. Past, 3, 51–64, doi:10.5194/cp-3-51-2007, 2007.

Wei, W. and Lohmann, G.: Simulated Atlantic multidecadal oscillation during the Holocene, J. Climate, in press, doi:10.1175/JCLI-D-11-00667.1, 2012.

Wei, W., Lohmann, G., and Dima, M.: Distinct modes of internal variability in the Global Meridional Overturning Circulation associated with the Southern Hemisphere westerly winds, J. Phys. Oceanogr., 42, 785–801, doi:10.1175/JPO-D-11-038.1, 2012.

Wolff, E. W., Fischer, H., and Röthlisberger, R.: Glacial terminations as southern warmings without northern control, Nat. Geosci., 2, 206–209, doi:10.1038/ngeo442, 2009.

CPD
8, 3015–3041, 2012

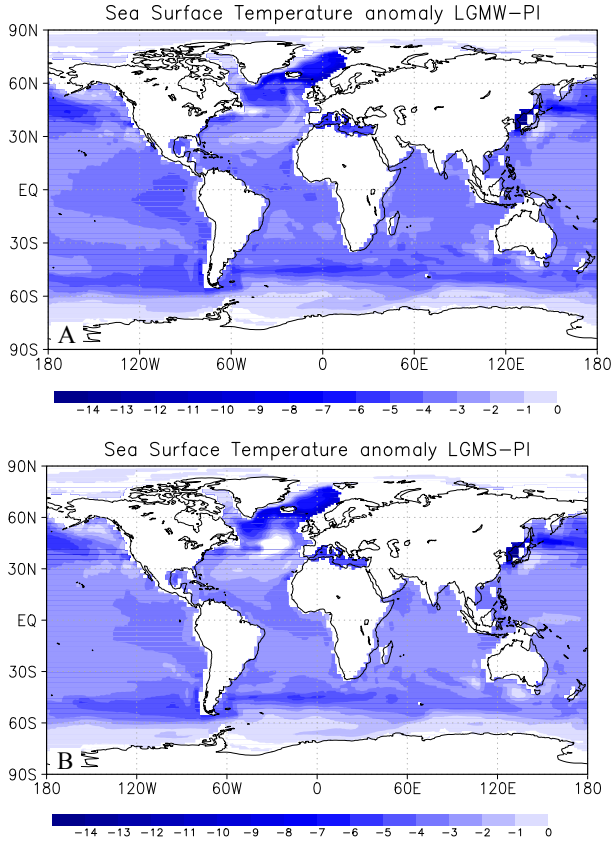

Fig. 1. Anomaly of sea surface temperature (SST) in LGMW **(A)** and LGMS **(B)** compared with PI. Unit: ˚C.

CPD
8, 3015–3041, 2012

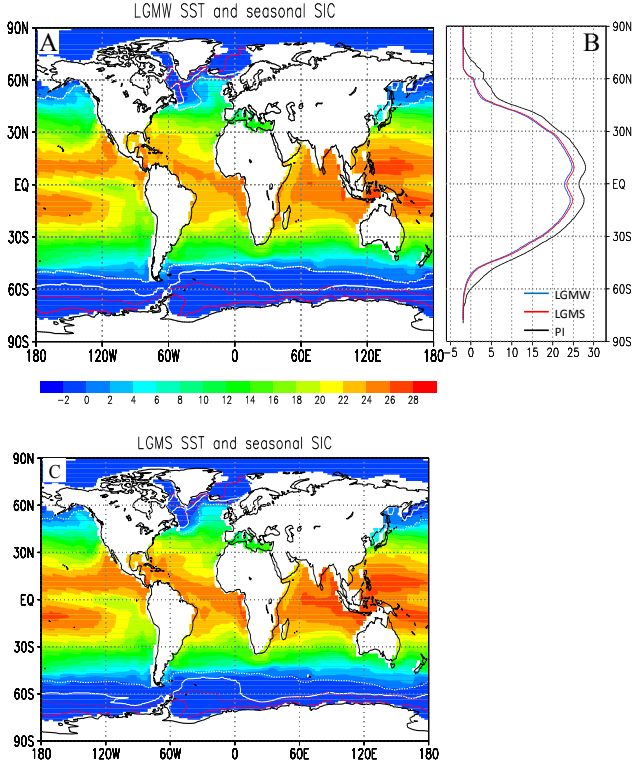

Fig. 2. Annual mean of sea surface temperature (SST, unit: ˚C, shaded) and seasonal sea ice concentration (SIC, unit: %, contour) in the LGMW **(A)** and LGMS **(C)**. The white lines represent winter for each hemisphere, while the red for summer. The dashed lines indicate 15 % SIC, and solid lines 90 % SIC. **(B)** Zonal mean of global SST in PI (black), LGMW (blue) and LGMS (red).

CPD
8, 3015–3041, 2012

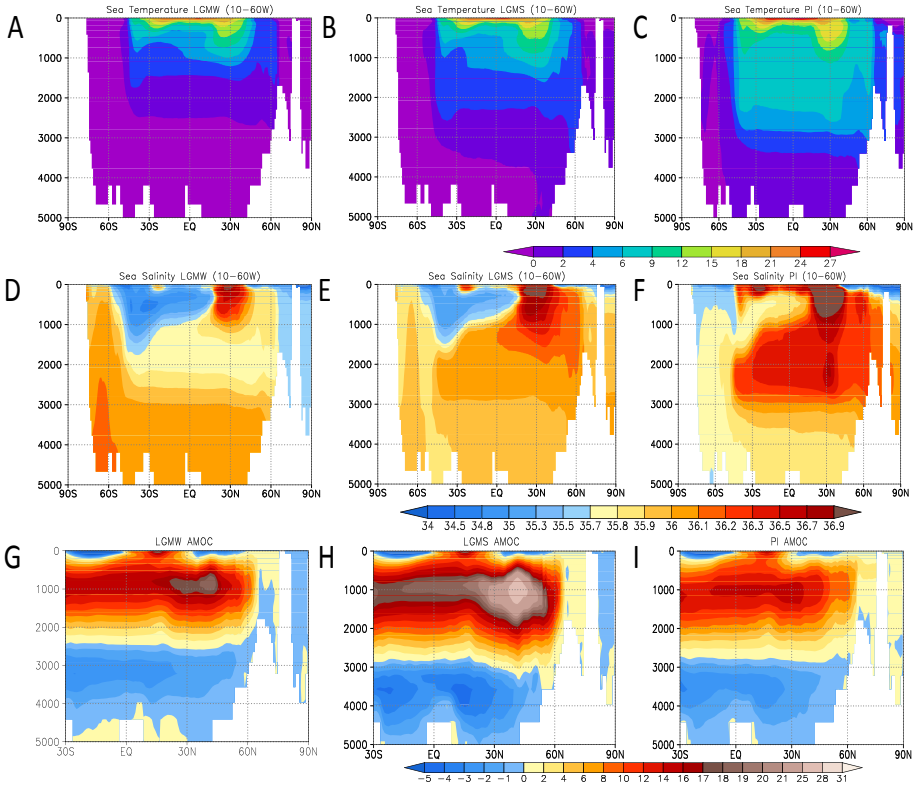

Fig. 3. Meridional section of zonal mean temperature (**A–C**, unit: ˚C), salinity (**D–F**, unit: psu) and Atlantic Meridional Overturning Circulation (**G–I**, unit: Sv (10^6 m^3 s^{-1})) in the Atlantic basin. For panel **(F)**, we added 1 psu to the salinity field for the better comparison with glacial salinity structure.

CPD
8, 3015–3041, 2012

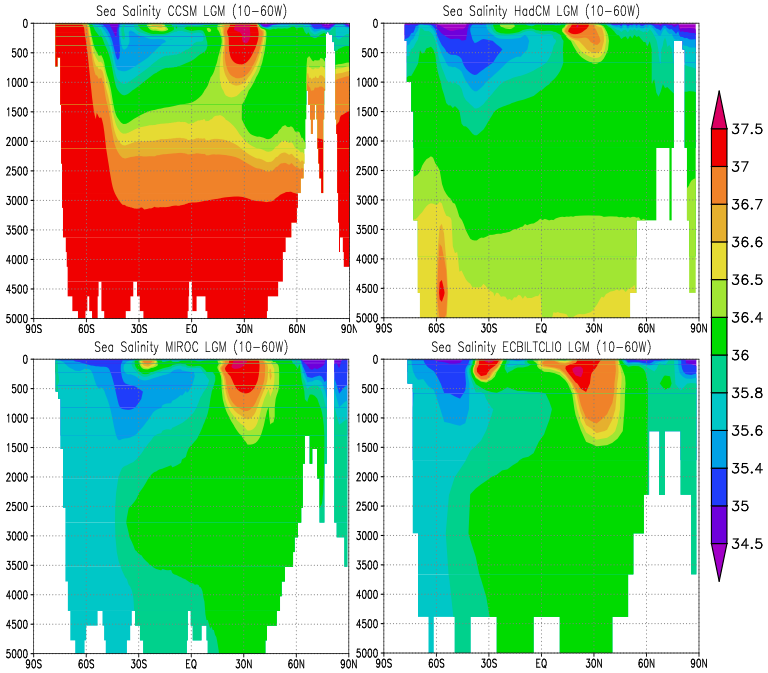

Fig. 4. Meridional section of zonal mean salinity in Atlantic Basin for PMIP2 models (i.e. CCSM, Otto-Bliesner et al., 2006; HadCM, Gordon et al., 2000; MIROC, Hasumi and Emori, 2004; and ECBilt-CLIO, Weber et al., 2007). The stratification in CCSM and HadCM is comparable with reconstruction (Otto-Bliesner et al., 2007), while the ocean structure in MIROC and ECBilt-CLIO is more like to present day with the saltiest deep-water mass in the North Atlantic. According to their salinity structure, one can divide the PMIP2 models into two main classes which are related to a highly stratified ocean, but weaker AMOC (as our LGMW) and weaker stratified, but stronger AMOC (LGMS).

CPD
8, 3015–3041, 2012

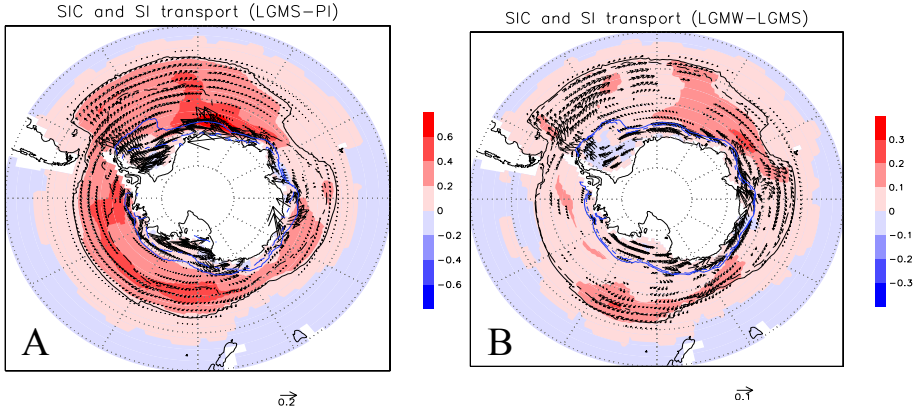

Fig. 5. (A) Anomaly of climatology SIC (%, shaded) and Sea Ice Transport ($m^2 s^{-1}$, vector, the scale is indicated by the black arrow below the panels) between LGMS and PI. Black contour represent 15 % SIC, while blue for 90 % SIC. Solid indicates SIC in LGMS, dashed for PI. **(B)** same as **(A)**, but for LGMW and LGMS. In our LGM runs, the extensive SIC and SIC export contribute to enhanced brine rejection which is of great importance to maintain the AABW formation during the LGM, consistent with Shin et al. (2003).

CPD
8, 3015–3041, 2012

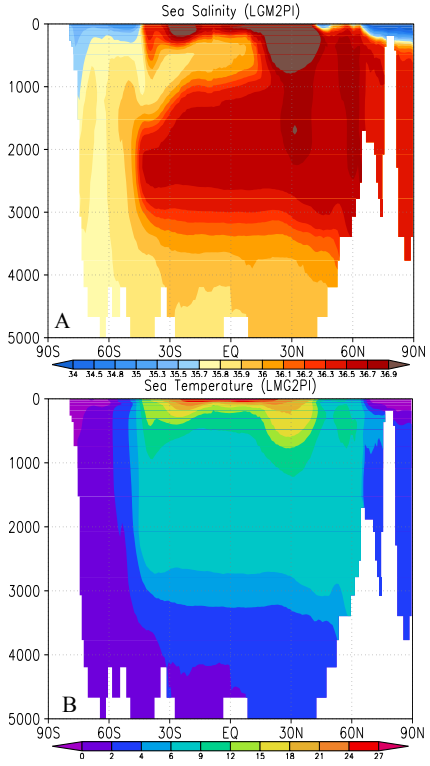

Fig. 6. Meridional section of zonal mean temperature **(A)** and salinity **(B)** in Atlantic basin in LGM2PI. LGM2PI which was imposed the same boundary condition as our control run but was initialized from the glacial ocean and was performed for 3000 yr. The last 100-yr average represents the corresponding climate state in LGM2PI. It is pronounced that the oceanic structure is almost the same as PI, indicating that pre-industrial simulation is insensitive to the initial ocean condition and emphasizing that initial ocean-dependent feature is unique for LGM simulation.

CPD
8, 3015–3041, 2012

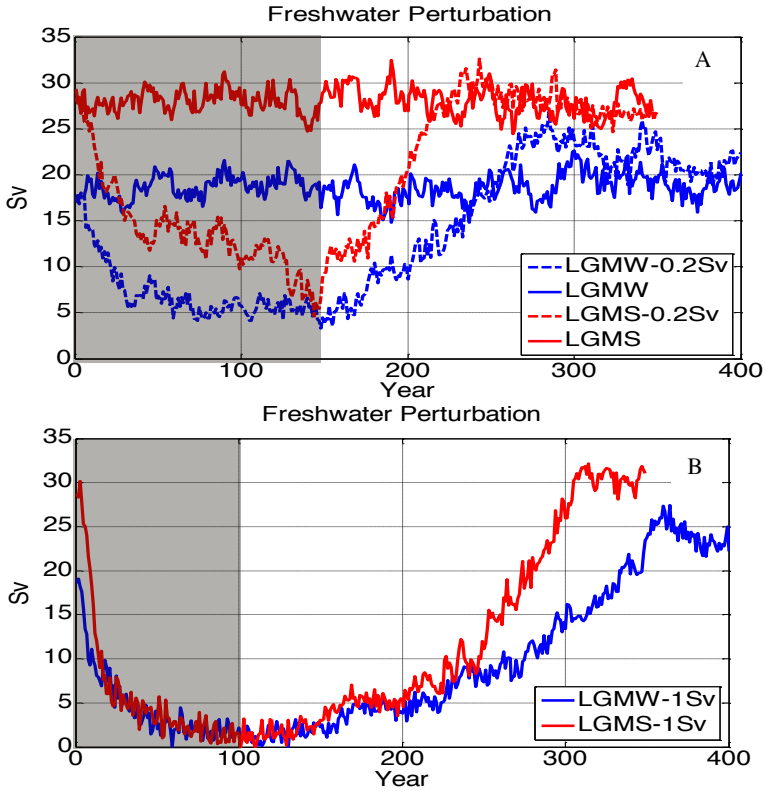

Fig. 7. Time series of AMOC in 0.2 Sv (**A**: FWP lasts for 150 yr) and 1 Sv (**B**: FWP lasts for 100 yr) hosing experiments of LGMW (blue) and LGMS (red). In **(A)**, the solid lines represent the LGM control runs, and dashed line for hosing experiments. In **(B)**, only hosing experiments were shown. Despite of the different amount of FWP, the transition between these two LGM states is not triggered. In addition, robust overshoot of AMOC was only found in LGMW experiments (Fig. 8).

CPD
8, 3015–3041, 2012

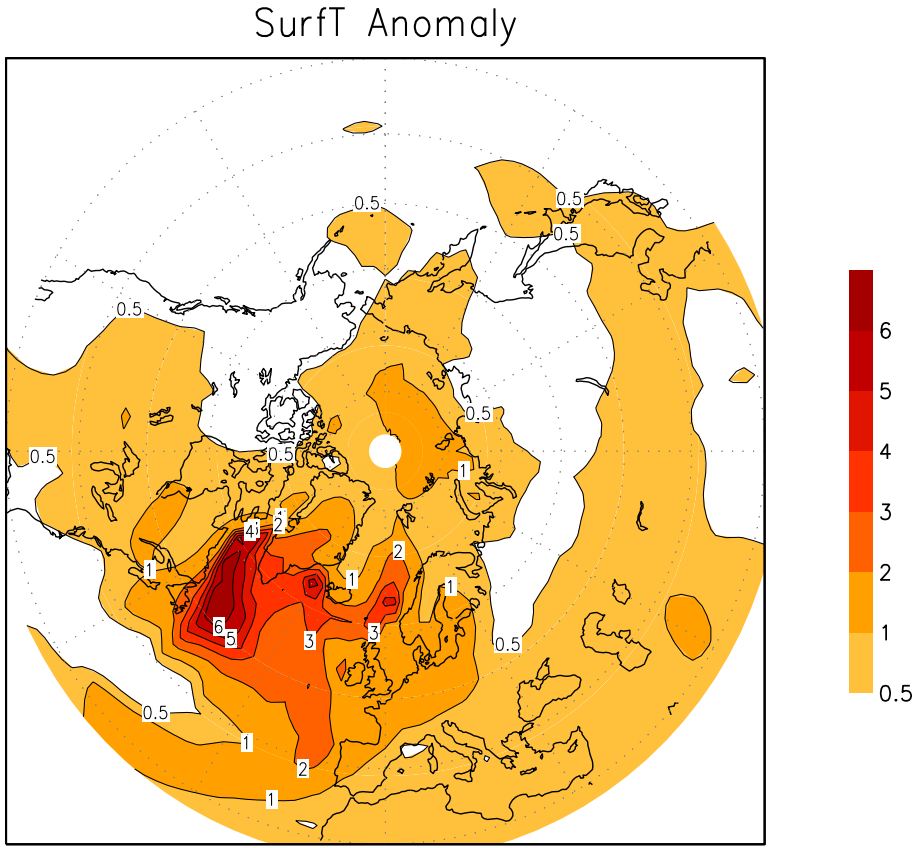

Fig. 8. Excess surface temperature increase related to the overshoot of the AMOC (270th–300th yr) in LGMW-0.2Sv. The pronounced temperature increase relative to LGMW in the North Hemisphere is up to 6.8 °C at convection sites of the North Atlantic.

CPD
8, 3015–3041, 2012

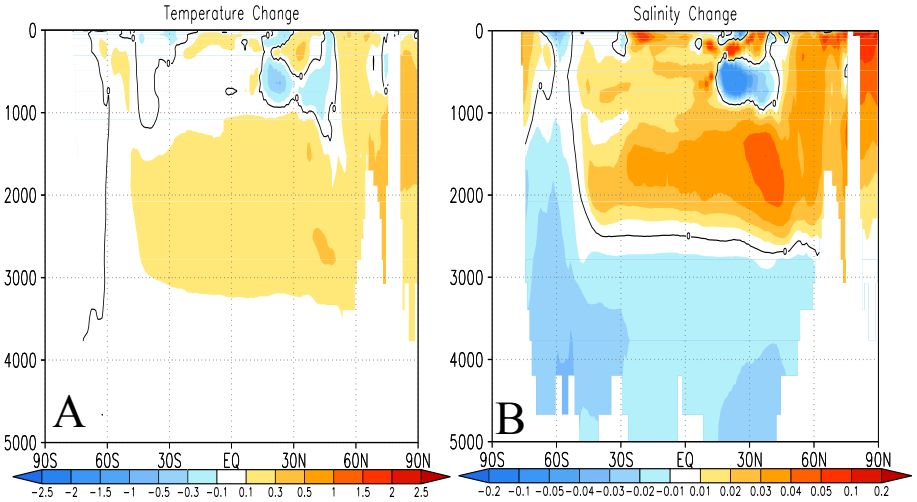

Fig. 9. Changes of zonal means of **(A)** sea temperature (°C) and **(B)** salinity (psu) in Atlantic basin after 500 yr in LGMW. Salinity of AABW is about 0.02 psu fresher, meanwhile GNAIW becomes 0.1 °C warmer and 0.03 psu saltier after 500 yr. According to the underlying trend, it would take approximately another 5000 yr to replace the salty AABW in the LGMW and to convert it to the LGMS-like Ocean.

CPD
8, 3015–3041, 2012

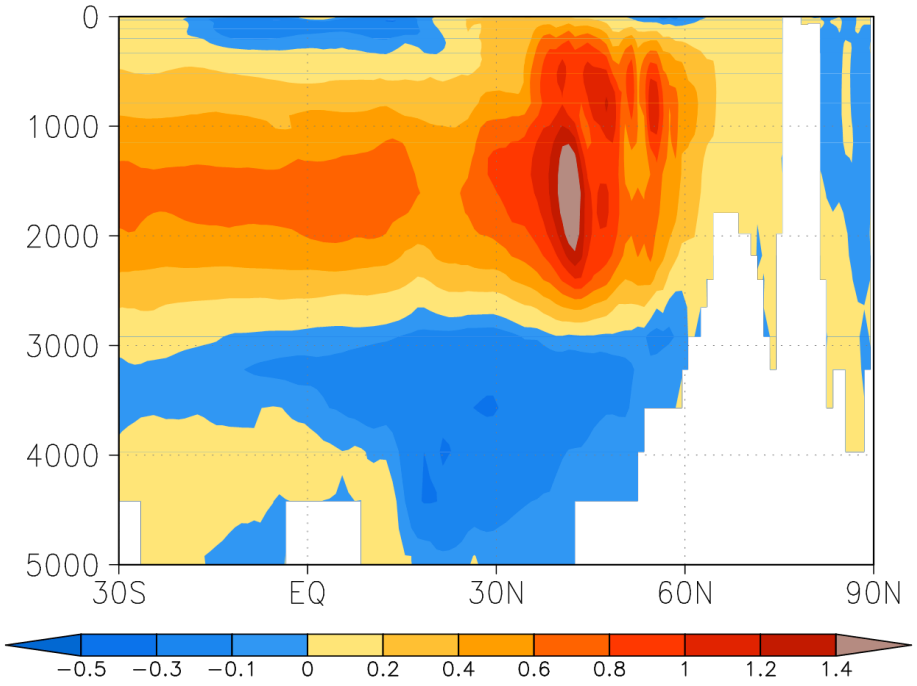

Fig. 10. Change in the AMOC (unit: Sv) after 500 yr in LGMW. Due to a weakened stratification resulting from the persistent upwelling in the Southern Ocean (Fig. 9), the AMOC which is sensitive to the stratification (Knorr and Lohmann, 2007), slowly increases with time.

CPD
8, 3015–3041, 2012